The Astrophysical Journal, 574:1059–1065, 2002 August 1

SOLAR SUBMILLIMETER AND GAMMA-RAY BURST EMISSION

P. Kaufmann,[1,2] J.-P. Raulin,[1] A. M. Melo,[1] E. Correia,[1] J. E. R. Costa,[1] C. G. Giménez de Castro,[1]
A. V. R. Silva,[1] M. Yoshimori,[3] H. S. Hudson,[4] W. Q. Gan,[5] D. E. Gary,[6] P. T. Gallagher,[6,7]
H. Levato,[8] A. Marun,[8] and M. Rovira[9]
Received 2001 November 23; accepted 2002 April 4

ABSTRACT

Solar flare emission was measured at 212 GHz in the submillimeter range by the Submillimeter Solar Telescope in the 1.2–18 GHz microwave range by the Owens Valley Solar Array and in the gamma-ray energy range (continuum) by experiments on board the *Yohkoh* (>1.2 MeV) and *Shenzhou 2* (>0.2 MeV) satellites. At the burst onset, the submillimeter and microwave time profiles were well correlated with gamma rays to the limit of the temporal resolution ($\leq$10 s). At 212 GHz, fast pulses (<1 s), defined as time structures in excess of the bulk emission, were identified as the flux increased. Their spatial positions were scattered by tens of arcseconds with respect to the main burst emission position. Correlation of submillimeter emission with gamma-ray fast time structures shorter than 500 ms is suggested at the gamma-ray maximum. The time variation of the rate of occurrence of the submillimeter rapid pulses was remarkably well correlated with gamma-ray intensities in the energy range (>1.2 MeV), attaining nearly 50 pulses per minute at the maximum. These results suggest that gamma rays might be the response to multiple rapid pulses at 212 GHz and might be produced at different sites within the flaring region.

Subject headings: gamma rays: bursts — Sun: flares

1. INTRODUCTION

The interaction of ultrarelativistic electrons (>MeV) accelerated during solar flares with the ambient magnetic field is expected to produce synchrotron emission in the submillimeter wavelength range together with gamma-ray continuum emission because of bremsstrahlung and line emission from nucleonic interactions in dense regions of the solar atmosphere (see, e.g., Ramaty et al. 1994; Trottet et al. 1993; Rieger, Treumann, & Karlicky 1999; Chupp 1995 and references therein). Diagnostics of flares in these energy ranges are thus important for understanding the origin of acceleration processes in solar flares.

The first submillimeter-wave bursts detected with the new solar submillimeter-wave telescope (SST) at El Leoncito revealed the presence of numerous rapid pulses (100–300 ms) with fluxes more intense at 405 GHz than at 212 GHz (Kaufmann et al. 2001b). The count rates varied approximately with the overall time-integrated Hα and soft X-ray emissions. The weak, slow (4 minute), nonthermal bulk component was later identified at submillimeter wavelengths and interpreted in the context of synchrotron emission of $\geq$6 MeV electrons (Trottet et al. 2002).

Simultaneous observations of a burst in the submillimeter and gamma-ray ranges were obtained for the first time on 2001 April 6. They corresponded to a *GOES* X5.6 class event, which occurred in the solar NOAA Active Region 9415, located at about S21°, E31°, at approximately 19:10–20:00 UT, as reported by the NOAA Space Environment Center and Solar-Geophysical Data bulletins. The performance of the new SST, located in El Leoncito, San Juan, Argentina, has been considerably improved after undergoing repairs, tests, and adjustments (Kaufmann et al. 2001a). It has two focal plane arrays: one has two 405 GHz feed horns and radiometers, receiving one plane of polarization, and another has four 212 GHz feed horns and radiometers, receiving the orthogonal plane of polarization. All six radiometers operate simultaneously, with the shortest time resolution of 1 ms. In Figure 1 we show the SST beams projected on NOAA AR 9415 in a *SOHO* Michelson Doppler Imager (MDI) magnetogram for 2001 April 6, where the half-power beam-widths were 4′ (beams 1–4 at 212 GHz) and 2′ (beams 5 and 6 at 405 GHz). Hard X-ray and gamma-ray continuum observations were obtained by two experiments. One is on board the recently launched Chinese *Shenzhou 2* satellite containing a bismuth germinate oxide (BGO) crystal scintillation detector 7.6 cm in diameter sensitive to the photon energies in several bands in the range 0.2–10 MeV, with best-sampling time resolution of 87 ms (Zhang, Tang, & Chang 2001). We also used the Hard X-Ray and Gamma-Ray Spectrometers (HXS and GRS, respectively), part of the Wide Band Spectrometer (WBS) experiment on the Japan/US/UK *Yohkoh* satellite, sensitive to photon energies in several energy bands in the range 25–830 KeV (for HXS) and in the range 0.27–100 MeV (for GRS) (Yoshimori et al. 1991). The GRS has two 7.6 cm

[1] CRAAM/CRAAE, Universidade Presbiteriana Mackenzie, Rua da Consolação 896, SP 01302-907 São Paulo, Brazil.
[2] Part-time researcher at CCS, UNICAMP, SP 13083-970 Campinas, Brazil.
[3] Rikkyo University, Tokyo 171-8501, Japan.
[4] Center for Astrophysics and Space Science, University of California at San Diego, La Jolla, CA 92093-0354.
[5] Purple Mountain Observatory, National Astronomical Observatories, Chinese Academy of Sciences, Nanjing, Jiangsu 210008, China.
[6] Physics Department, New Jersey Institute of Technology, Newark, NJ 07012.
[7] Current Address: Emergent Information Technologies, Inc., NASA Goddard Space Flight Center, Code 682, Greenbelt, MD 20771.
[8] Complejo Astronomico El Leoncito (CASLEO), Casillo de Correo 467, Avenue Espana 1512 Sur, 5400 San Juan, Argentina.
[9] Instituto de Astronomia y Física del Espacio (IAFE), Buenos Aires, Argentina.

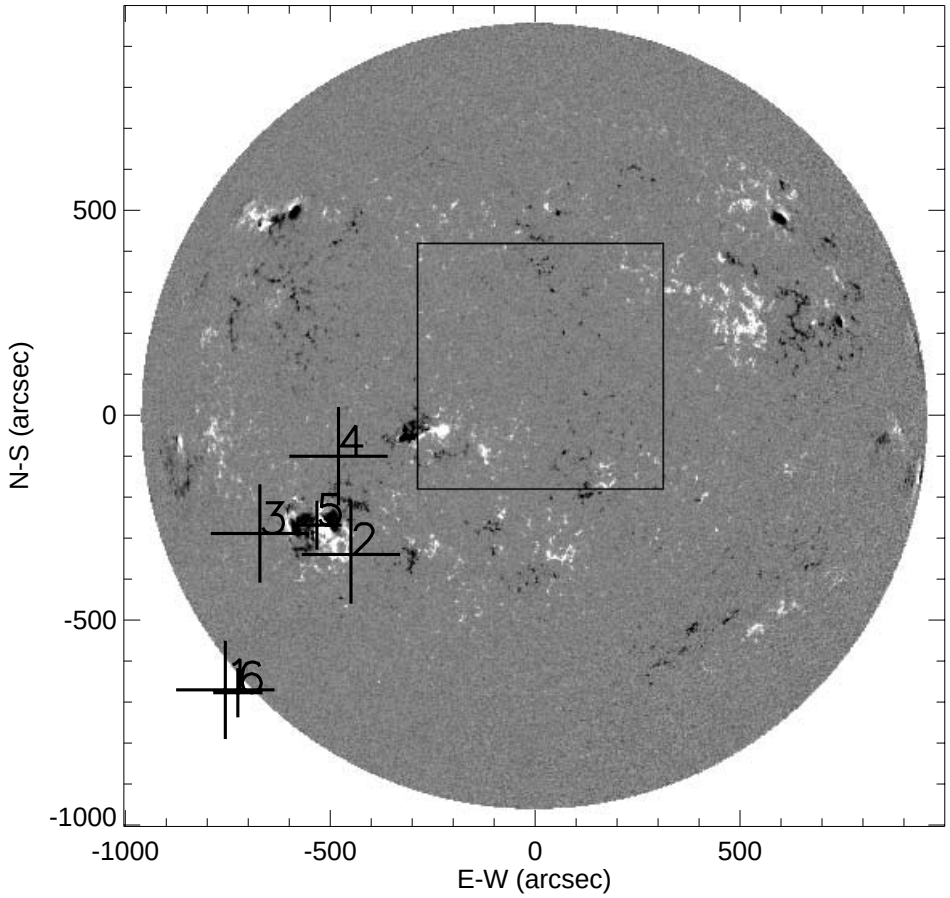

FIG. 1.—SST beams projected on a *SOHO* MDI solar magnetogram for 2001 April 6. Beam 5 (405 GHz) and partially overlapping beams 2, 3, and 4 (212 GHz) were on NOAA AR 9415, while beam 1 (212 GHz) and beam 6 (405 GHz) were about 7′ from the cluster.

diameter BGO scintillation detectors with best time resolution of 250 ms.

Microwave spectral observations were obtained by the Owens Valley Solar Array (OVSA) in the range 1.2–18 GHz, covering nearly 40 frequencies with spectral data obtained with 8 s time resolution. OVSA instrument details can be found in Hurford, Read, & Zirin (1984) and Gary & Hurford (1998).

2. SUBMILLIMETER, MICROWAVE, AND GAMMA-RAY EMISSION

The atmospheric attenuation was exceptionally high at the time of the 2001 April 6 burst observations. The optical depths derived from solar maps, taken 15 minutes before the event, were 1.2 at 212 GHz and 4.3 (i.e., practically opaque) at 405 GHz. In Figure 2 we show the OVSA 18 GHz, SST 212 GHz, and *Yohkoh* WBS 0.53–17.1 MeV time profiles for the event using a compressed timescale. The 212 GHz antenna temperatures were corrected for sky opacity at the elevation angle of the Sun during the burst observation (37°.5) and for the source position with respect to beams 2, 3, and 4, using the multiple-beam correlation technique (Giménez de Castro et al. 1999 and references therein). The submillimeter flux scale as derived from the antenna temperatures, corrected for the beam displacement factors and antenna aperture efficiencies, is about 20% for beams 2, 3, and 4 (212 GHz) and about 15% for beam 5 (405 GHz). The approximate total systematic uncertainty of the flux scale, taking into account correction errors caused by the high value of atmospheric absorption and the efficiency measurement inaccuracies, might be as large as about $\pm 50\%$ for the present determinations. We obtained about 5800 sfu ($1\ \mathrm{sfu} = 10^{-22}\ \mathrm{W\ m^{-2}\ Hz^{-1}}$) for the 212 GHz main bulk emission maximum at about 1918–1919 UT, while the 405 GHz detection was restricted to an upper limit of 6700 sfu defined by the noise level. The submillimeter maximum occurred during the calibration of SST. It seems to correspond to the 18 GHz maximum of about 9000 sfu, which is delayed by about 2 minutes with respect to the gamma ray, showing a rapid decay followed by a postburst increase.

Figure 3 shows the time-expanded time profiles of the burst onset stage for the main gamma-ray peaks, detected by the experiments on the *Shenzhou 2* and *Yohkoh* satellites with the 212 GHz emission. It is clear that there is a temporal correlation of features in high-energy X-rays, in gamma rays, and at 212 GHz within the time resolution of the X- and gamma-ray count rate readings in these plots ($\leq$10 s). The continuum nature of gamma-ray emission was confirmed by the inspection of the gamma-ray spectrum derived from the WBS/GRS spectrometer, showing no evidence of nuclear line contribution.

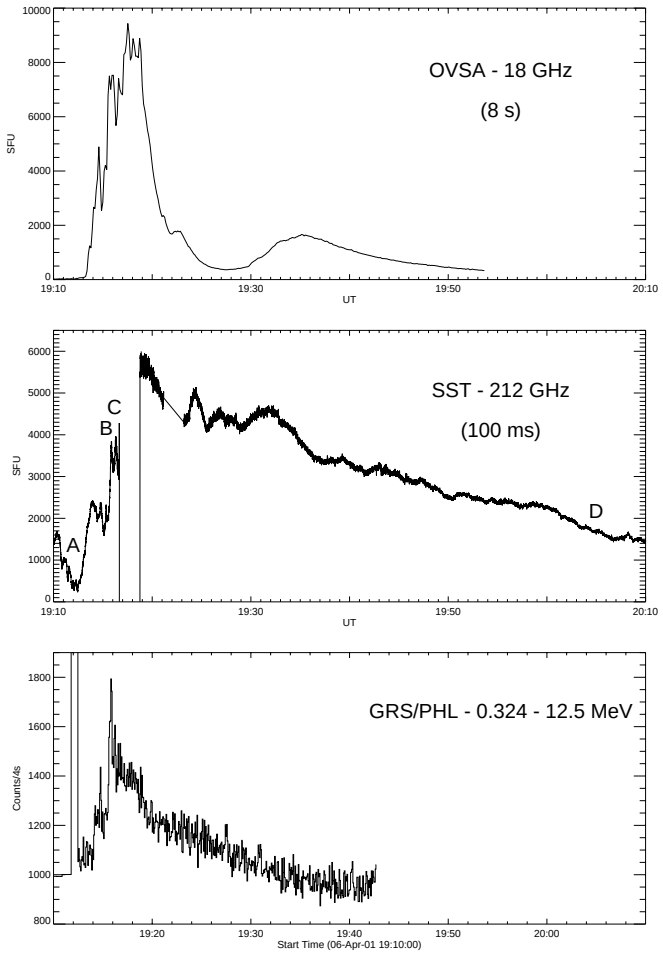

FIG. 2.—Time profiles in compressed timescale. *Top*, OVSA 18 GHz, 8 s time resolution. *Middle*, SST 212 GHz 100 ms data, in solar flux units. *Bottom*: *Yohkoh* 0.324–12.5 MeV gamma rays, in counts per 4 s. The 10 s expansion samples at times labeled A–D are shown in Fig. 4.

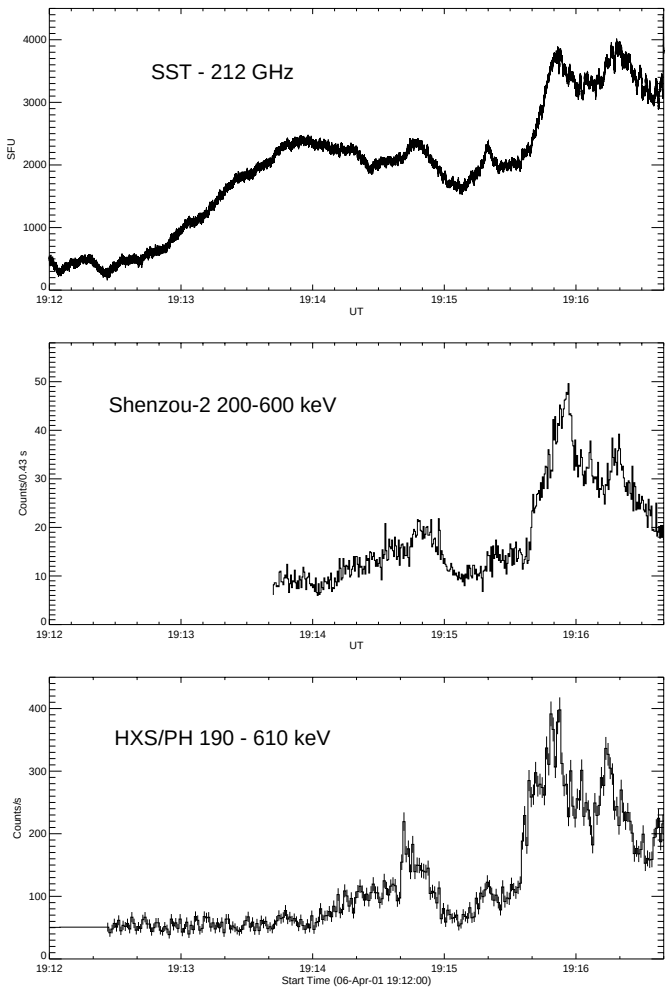

FIG. 3.—Expanded time section of the burst for the rise phase at 212 GHz (*top*) and gamma rays obtained by the *Shenzhou 2* (*middle*) and *Yohkoh* (*bottom*) satellites.

Ten second 212 GHz emission samples have been chosen before the burst onset (*A*), at the gamma-ray maximum (*B*) and (*C*), and later in the decay phase (*D*). They are shown in Figure 4 corresponding to the labels marked in Figure 2. Rapid, large, and frequent subsecond spikes appear superposed as the main emission flux increase. The relative amplitude of the rapid spikes is 200–400 sfu. The count rates were determined and are discussed in § 3.

The spatial position of the 212 GHz emission, determined by correlating the intensities of beams 2, 3, and 4 using the multiple-beam technique (e.g., Gimenez de Castro et al. 1999 and references therein) has shown that the main emission component remains nearly stable during the maximum phase, to within the 10″ relative uncertainty (see Fig. 5). The positions in space of the superposed fast structures of samples B and C are shown in Figure 5. There is a clear dispersion of their positions extending up to 40″ with respect to the underlying main emission source position. Spatial scattering of the same order has been found at longer millimeter wavelengths (48 GHz) for impulsive components in complex bursts, each one containing numerous superposed fast time structures (Correia et al. 1995; Raulin et al. 1998).

The OVSA 18 GHz flux at about the burst maximum was about 9000 sfu. The spectral shape in the 1.2–18 GHz frequency range was time-varying. Three representative spectra are shown in Figure 6. At the beginning of the event, 19:12–19:14 UT, the turnover frequency was at about 10 GHz. At the time of the gamma-ray maximum emission, 19:15–19:16 UT, the spectrum was continuously increasing with frequency with a spectral index of +1.2. At the time of maximum microwave and submillimeter emissions, at about 19:17–19:19 UT, there is again a flattening for the upper frequencies with a turnover at about 11 GHz and flux level of 9000 sfu. These results suggest that the burst bulk maximum emission presented a slow decay over the entire range of frequencies, from 18 to 212 GHz. The latter suggestion is similar to another example of a solar burst with a flat spectrum extending up to 86 GHz reported by White et al. (1992).

3. SUBMILLIMETER SPIKE REPETITION RATES AND GAMMA-RAY EMISSION

In Figure 7 we compare the time profiles of the 212 GHz flux, the fast-spike occurrence rate, and gamma rays (>1.2 MeV). Pulses were counted based on a peak-finding algorithm (Raulin et al. 1998). Only the larger pulses, exceeding 3 σ above the noise, or about 80 sfu, were selected. There is a

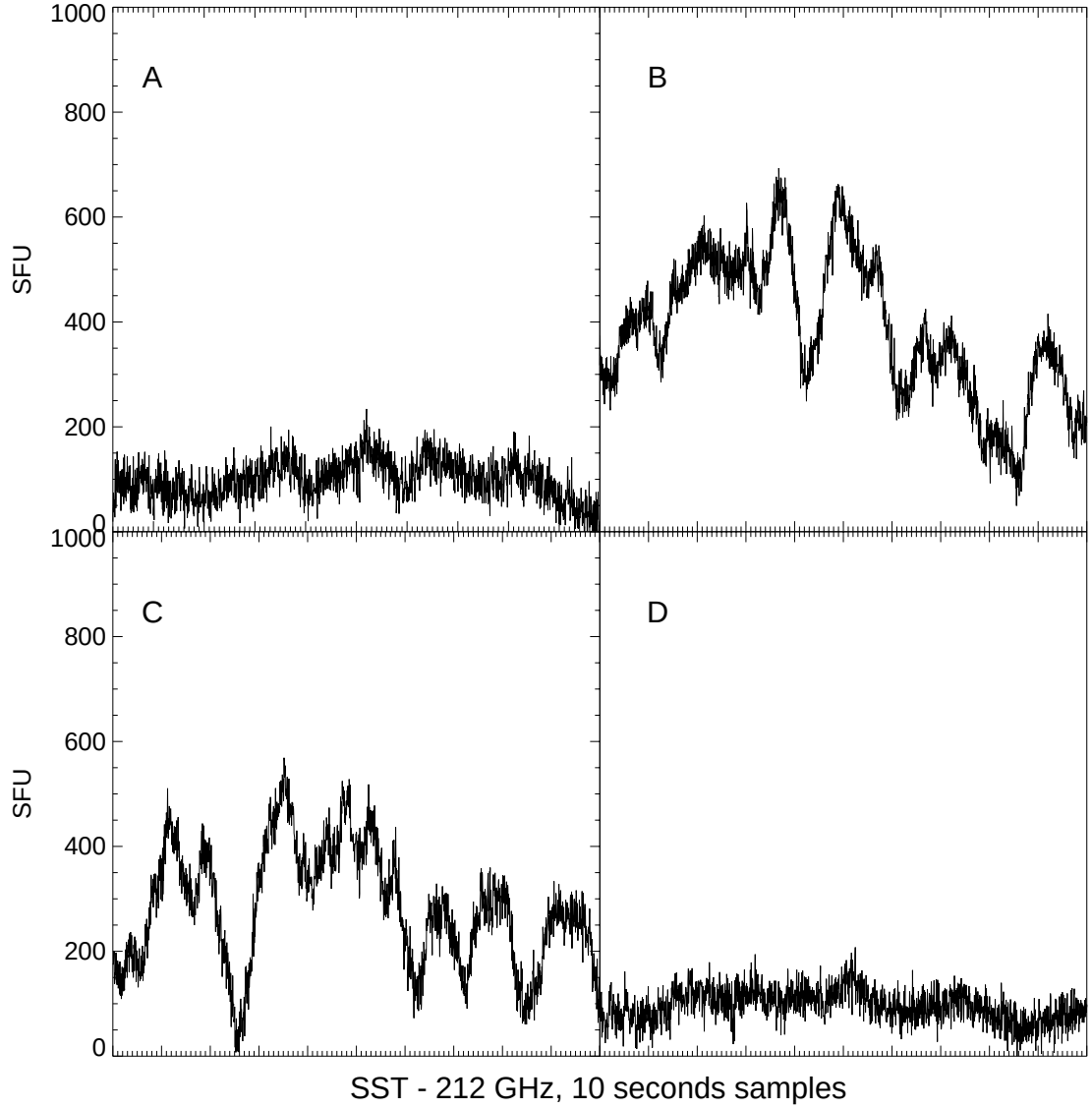

FIG. 4.—Represents 10 s time expansions for 212 GHz emission, 5 ms time resolution, in solar flux units relative to the underlying levels, for the times labeled A–D in Figs. 2 and 3.

remarkable correlation between the gamma rays (>1.2 MeV) and submillimeter pulse rate profiles during the whole event. The count rates of 212 GHz pulses decrease faster than the bulk emission at 212 GHz.

The detailed comparison of the 212 GHz rapid spikes and the gamma-ray time structures is limited by the low significance of the gamma-ray count rate readings. A meaningful association of fast time structures in the two ranges is suggested for the gamma-ray peak, labeled B in Figure 2. Panel B of Figure 4 is reproduced in Figure 8 with a 0.5 s running mean, together with gamma-ray counts per 0.5 s for the energy bands 0.24–1.04 MeV (P11 detector) and 1.04–5.47 MeV (P12 detector). The correspondences for the major time structures are very suggestive and qualitatively comparable to the results obtained for subsecond pulses observed at lower hard X-ray ranges and millimeter waves (Takakura et al. 1983; Zodi Vaz et al. 1985). Cross-correlation between millimeter-wave subsecond time structures and hard X-rays detected by BATSE on board the *Compton Gamma Ray Observatory* (*CGRO*) has provided significant coefficients with time coincidence to the limit time resolution of 64 ms for the energy ranges 25–62, 62–111, and 111–325 keV (Kaufmann et al. 2000). Cross-correlation between metric radio type III time structures and ≥25 keV X-rays detected by the hard X-ray burst spectrometer (HXRBS) experiment on board the *Solar Maximum Mission* (*SMM*) satellite has shown that 0.2–2.0 s duration time structures were correlated with a typical delay of about 0.4 s of radio with respect to the X-rays (Aschwanden et al. 1995). To confirm the association between the fast time structures at the gamma-ray peak and the 212 GHz structures, shown in Figure 8, we cross-correlated the 10 s data sets, applying the same method as in Kaufmann et al. (2000), and show the results in Figure 9. The cross-correlation coefficients, in relative units, are significantly larger for the peak of the event, in comparison to the coefficients obtained for the same cross-correlation done for another 10 s set of data taken at a later phase, in dashed lines (i.e., at 19:39:00–19:39:10 UT). The

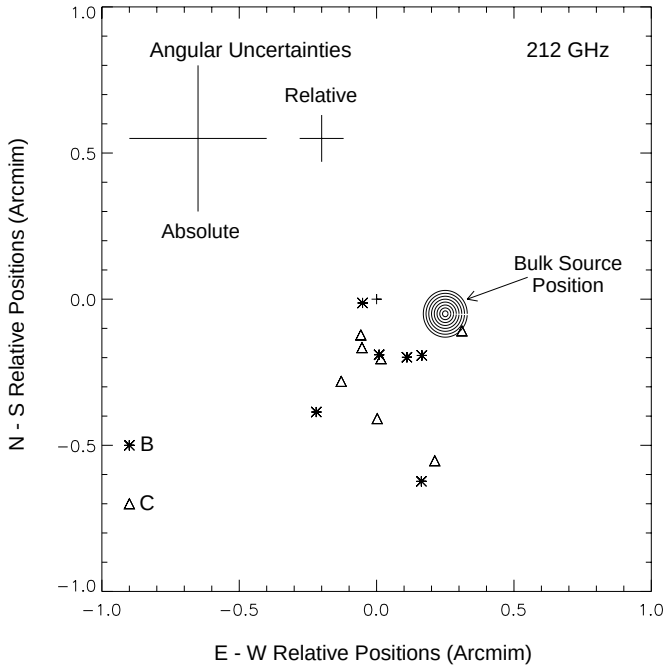

FIG. 5.—Spatial positions for the 212 GHz spikes shown in Fig. 4, panels B and C, with respect to the position of the maximum main emission component. The absolute and relative angular uncertainties are indicated.

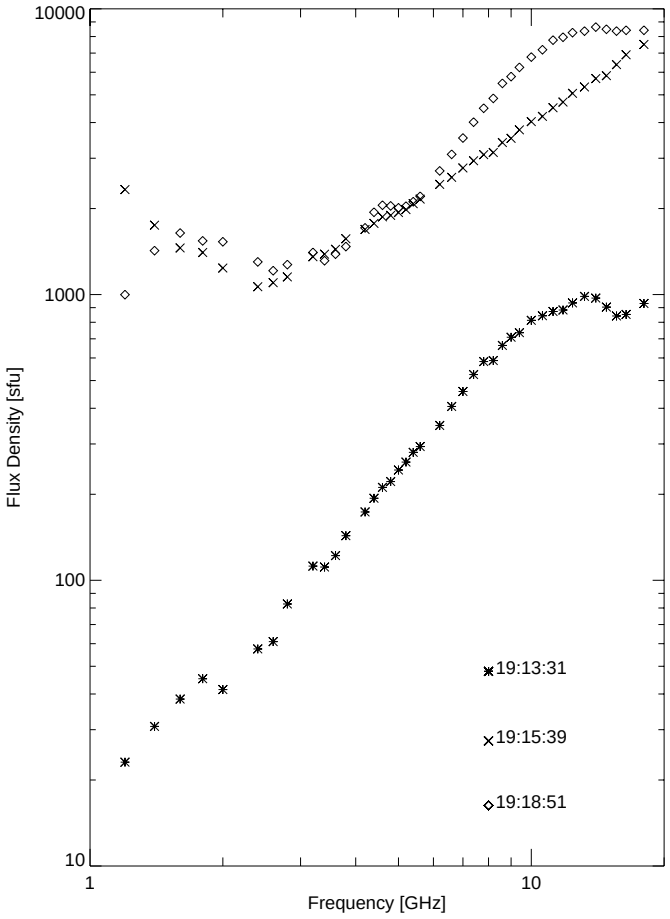

FIG. 6.—OVSA 1.2–18 GHz burst spectra for three different phases of the burst: at the beginning, at the gamma-ray maximum, and at the microwave and submillimeter maximum.

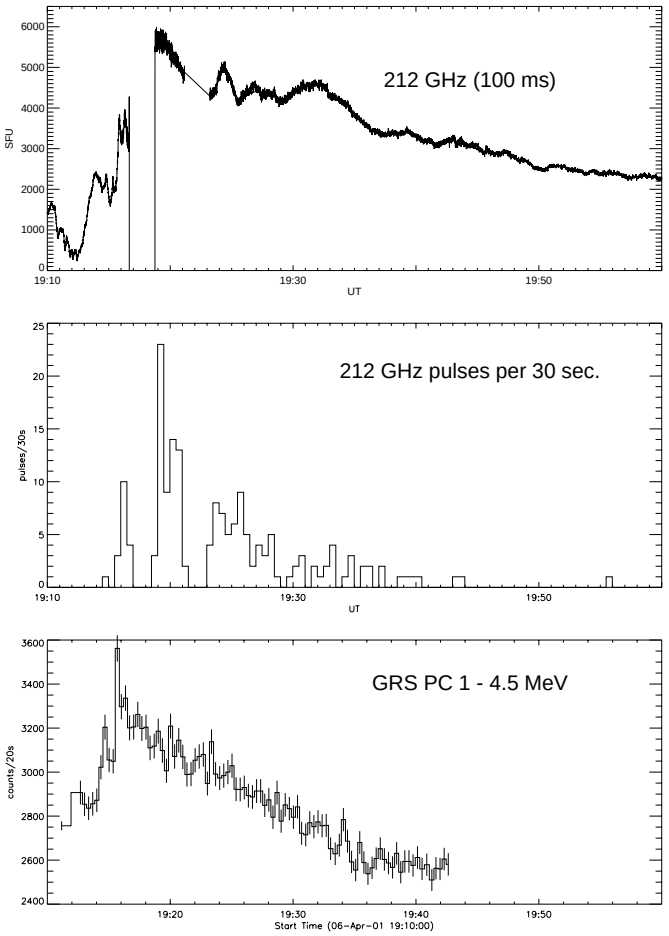

FIG. 7.—212 GHz pulse count rates with time (*middle*) compared to the 2001 April 6 burst 212 GHz compressed time profile (*top*) and to the *Yohkoh* GRS gamma ray (*bottom*). The 212 GHz spikes count rate time profile has a strikingly good correspondence with the higher energy gamma rays (>MeV) time profile.

cross-correlation plot for the peak of the event indicates a time coincidence with an uncertainty of about ±250 ms, resulting from the limited time resolution of the gamma-ray data.

4. CONCLUDING REMARKS

Simultaneous observations of a solar burst in the submillimeter range (212 GHz), microwaves (1.2–18 GHz), and high-energy X- and gamma rays (>1.2 MeV) have shown a good time correspondence during the rise phase of the event to better than 10 s. A correlation of better than ≈500 ms is suggested for the fast spikes at the gamma-ray maximum. There is an excellent correspondence between the 212 GHz fast-pulse count rates and the time profile above 1.2 MeV for the whole event. This property suggests that the observed gamma-ray emission is proportional to the number of pulses per unit time observed in the submillimeter range, which might then be signatures of the primary energetic injections. A similar relationship was found for burst emission in the centimeter-millimeter wave range, leading to the suggestion that the burst energies are proportional to the number of injections, quasi-quantized in energy (Kaufmann et al. 1980; Raulin et al. 1998). On the other hand, the correlation between hard X-rays, gamma rays, microwaves,

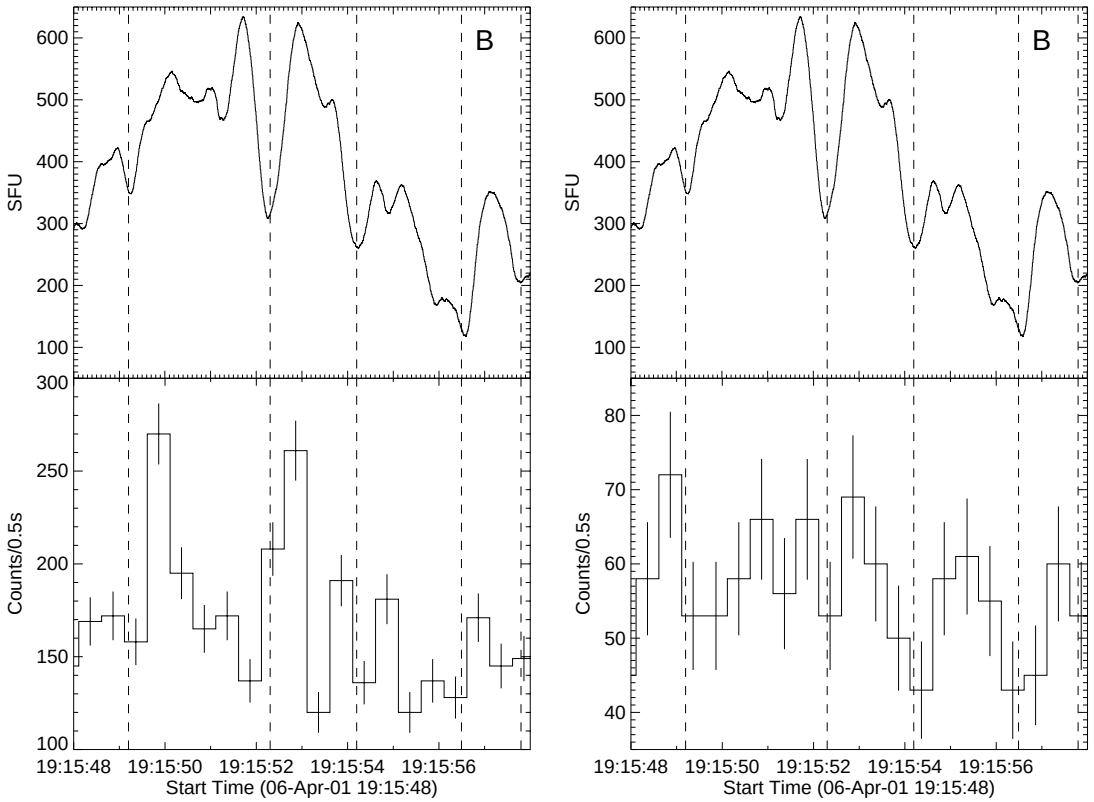

FIG. 8.—Direct comparison of spikes observed with 500 ms time resolution, as running means at 212 GHz (*top*) and at greater than 0.24 MeV (*left*) and greater than 1 MeV (*right*) gamma rays, for the gamma-ray maximum, label B (see Figs. 2, 3, and 4). Vertical lines indicate minima between submillimeter structures.

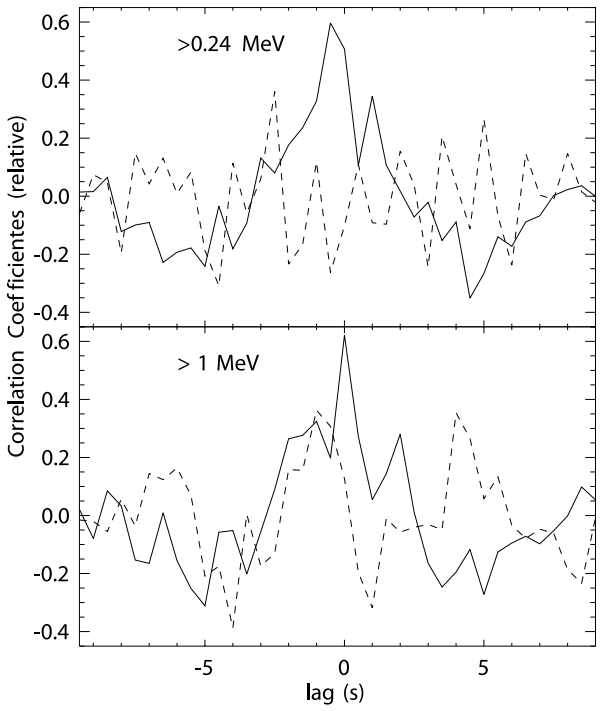

FIG. 9.—Cross-correlation of gamma-ray and 212 GHz data for the 10 s at the peak of the burst, shown in Fig. 8 (*solid line*) compared to the same correlation done at a later phase of the burst (19:39:00–19:39:10 UT, *dashed line*). The pronounced increase in the coefficients, nearly "in phase" within the 500 ms time resolution of the data, confirm the direct comparison of gamma-ray and 212 GHz fast time structures at the peak of the event shown in Fig. 8.

and submillimeter time profiles is less pronounced after the principal gamma-ray peak at 19:16 UT. Submillimeter and 18 GHz peaks are nearly 2 minutes later than the high-energy peaks. The decay phase is longer at submillimeter wavelengths compared to that of microwaves, and the latter present an extended postburst increase, not observed at gamma rays. This might indicate that radio emission reflects not only direct injection/precipitation of energetic particles (as gamma rays do) but also slower processes, such as transport, trapping, and diffusion.

The positions in space of the 212 GHz fast subsecond pulses were found to be scattered up to 40″ with respect to the position of the bulk emission source, suggesting that the primary energy release sites are also discrete in space, spread out over the bursting region. Very similar results were obtained for fast spikes observed superposed to millimeter-wave burst emissions (Correia et al. 1995; Raulin et al. 1998).

Electrons with energies $\geq$10 MeV are required to explain the intense microwave to submillimeter-wave burst bulk emissions with high turnover frequency and associated gamma rays (Ramaty et al. 1994; Trottet et al. 2002 and references therein). The flattening of the radio spectrum from about 10 to 212 GHz might be a realistic possibility, as found for one event observed up to 86 GHz (White et al. 1992). It might be explained by the composition of multiple synchrotron spectra produced throughout the burst duration (Hachenberg & Wallis 1961) or taking into account a number of source parameters for which a synchrotron self-absorption mechanism might have a major contribution (Ramaty & Petrosian 1972; Klein 1987).

New diagnostics are needed to provide more clues for the understanding of the fast pulses that are found superposed to the burst bulk emissions, when sensitivity and time resolution are available. They seem to become more pronounced in the submillimeter wave range. It would be interesting to combine this research with optical imaging with high cadence rates (such as described by Wang et al. 2000).

The authors are grateful for the support of CASLEO engineers and technicians at El Leoncito. This research was partially supported by Brazilian agencies FAPESP, contracts 99/06126-7, 01/03791-1, and CNPq, and Argentina agency CONICET. CRAAE is a joint center between Mackenzie, INPE, USP, and Unicamp.

REFERENCES

Aschwanden, M., Montello, M. L., Dennis, B. R., & Benz, A. O. 1995, ApJ, 440, 394
Chupp, E. L. 1995, in AIP Conf. Proc. 374, High Energy Solar Physics, ed. R. Ramaty, N. Mandzhavidze, & X. M. Hua (New York: AIP), 3
Correia, E., Costa, J. E. R., Kaufmann, P., Magun, A., & Herrmann, R. 1995, Sol. Phys., 159, 143
Gary, D. E., & Hurford, G. J. 1998, in Proc. Nobeyama Symposium, ed. T. S. Bastian, N. Gopalswamy, & K. Shibasaki (NRO Rep. 49; Nagano: Nobeyama Radio Obs.), 429
Giménez de Castro, C. G., Raulin, J.-P., Makhmutov, V. S., Kaufmann, P., & Costa, J. E. R. 1999, A&AS, 140, 373
Hachenberg, O., & Wallis, G. 1961, Z. Astrophys., 52, 42
Hurford, G. J., Read, R. B., & Zirin, H. 1984, Sol. Phys., 94, 413
Kaufmann, P., et al. 2001a, in Proc. 2001 SBMO/IEEE MTT-S International Microwave and Optoelectronics Conference, ed. J. T. Pinho, G. P. S. Cavalcante, & L. A. H. G. Oliveira (Belém: IEEE), 439
Kaufmann, P., et al. 2001b, ApJ, 548, L95
Kaufmann, P., Strauss, F. M., Opher, R., & Laporte, C. 1980, A&A, 87, 58
Kaufmann, P., Trottet, G., Giménez de Castro, C. G., Costa, J. E. R., Raulin, J.-P., Schwartz, R. A., & Magun, A. 2000, Sol. Phys., 197, 361
Klein, K.-L. 1987, A&A, 183, 341
Ramaty, R., & Petrosian, V. 1972, ApJ, 178, 241
Ramaty, R., Schwartz, R. A., Enome, S., & Nakajima, H. 1994, ApJ, 436, 941
Raulin, J.-P., Kaufmann, P., Olivieri, R., Correia, E., Makhmutov, V. S., & Magun, A. 1998, ApJ, 498, L173
Rieger, E., Treumann, R. A., & Karlicky, M. 1999, Sol. Phys., 187, 59
Takakura, T., Kaufmann, P., Costa, J. E. R., Degaonkar, S. S., Ohki, K., & Nitta, N. 1983, Nature, 302, 5906
Trottet, G., Raulin, J.-P., Kaufmann, P., Siarkowsky, M., Klein, K. L., & Gary, D. E. 2002, A&A, 381, 694
Trottet, G., Vilmer, N., Barat, C., Dezalay, J.-P., Talon, R., Sunyaev, R., Kuznetsov, A., & Terekhov, O. 1993, A&AS, 97, 337
Wang, H., Qiu, J., Denker, C., Spirock, T. J., Chen, H., & Goode, P. R. 2000, ApJ, 542, 1080
White, S. M., Kundu, M. R., Bastian, T. S., Gary, D. E., Hurford, G. J., Kucera, T., & Bieging, J. H. 1992, ApJ, 384, 656
Yoshimori, M., et al. 1991, Sol. Phys., 136, 69
Zhang, N., Tang, H. S., & Chang, J. 2001, Acta Astron. Sinica, 42, 351
Zodi Vaz, A. M., Kaufmann, P., Correia, E., Costa, J. E. R., Cliver, E. W., Takakura, T., & Tapping, K. F. 1985, in Rapid Fluctuations in Solar Flares, ed. B. R. Dennis, L. E. Orwig, & A. L. Kiplinger (NASA CP-2449; Washington: NASA), 171